

INNOVATIVE APPROACH TO HIGH-SPEED SPINNING USING A MAGNETICALLY-ELEVATED SPINNING RING

Faissal Abdel-hady, Yehia El Mogahzy, Sherif AbuElenin*, and Rabab Abdel-Kader

Textile Engineering Department, Auburn University, Auburn, AL 36849, U.S.A.

Abstract

We introduce a new concept of ring-spinning. The model system built on the basis of this concept is capable of producing yarns at a production rate of up to 4 times that of the traditional ring-spinning system. This is a direct result of a ring rotational speed of up to 40,000 rpm. This new concept is termed 'magnetic spinning', and it principally consists of a lightweight rotor suspended magnetically inside a fixed stator; the rotor can spin freely inside the stator. The stator is equipped with four magnetic actuators that always keep the rotor in its central position. The rotor in this configuration replaces the ring and traveller in the traditional spinning system. The system's concept and control analysis are discussed in this paper.

Key words:

ring-spinning, magnetic spinning, floating traveller, high-speed spinning, magnetic suspension

Introduction

In today's technology, many spinning systems are used commercially to produce spun yarns with a wide range of values of characteristics. Among these systems, ring spinning enjoys the greatest diversity and the highest quality levels. Other spinning systems such as rotor spinning, air-jet spinning, and friction spinning suffer inherent limitations that make them suitable for only narrow ranges of yarn count and twist levels [3, 10, 12]. However, the major limiting factor in ring spinning is their low production rate in comparison with all new spinning technologies. Typically, ring-spinning can only operate at a production speed of up to 30 m/min, while other systems producing comparable yarns (such as rotor spinning and air-jet spinning) can operate at production speeds of up to 250 m/min.

The low production rate in ring spinning is primarily attributed to the use of the ring/traveller system for twisting and winding. More specifically, it is attributed to the following factors [4, 6, 7, 9, 12]:

- The dependence of the yarn linear speed (or delivery speed) on the rotational speed of the traveller, or more precisely on the rate of twist insertion;
- The continuous need to stabilise yarn tension during spinning, and the significant dependence of this stability on the traveller speed;
- The impact of traveller speed on the performance of fibres in the spinning triangle, and in the ring/traveller zone.

The common aspect in the above factors is traveller speed, and more specifically, the ring/traveller system. In this region, a metallic traveller with a small mass, m , rotates around a metallic ring of a constant radius, r . At the point of ring/travel contact many forces are involved, as previously analysed by a number of investigators. These include yarn tension T_1 , imposed by the balloon region, yarn tension T_2 , imposed by the winding mechanism, a reaction force N , a friction force F in the ring plane, and tangential to the ring. These forces are illustrated in Figure 1. Different equations governing the interaction of these forces were developed by Batra et al [4, 5] and Skendderi et al [13].

In practice, the different forces involved in the ring/traveller system result in great limitations, not only on the production rate of ring spinning but also in relation to yarn quality. Any opportunity to increase productivity in ring spinning must be achieved by means of an increase in traveller speed. Since the principle of ring-spinning dictates continuous ring-traveller contact, high traveller speed will result in the traveller burning out due to the frictional heat initiated during traveller rotation. In addition, the centrifugal force acting on the traveller results in a gradual wearing out of the traveller, which can greatly influence the yarn surface's integrity, leading in turn to high hairiness and yarn imperfections.

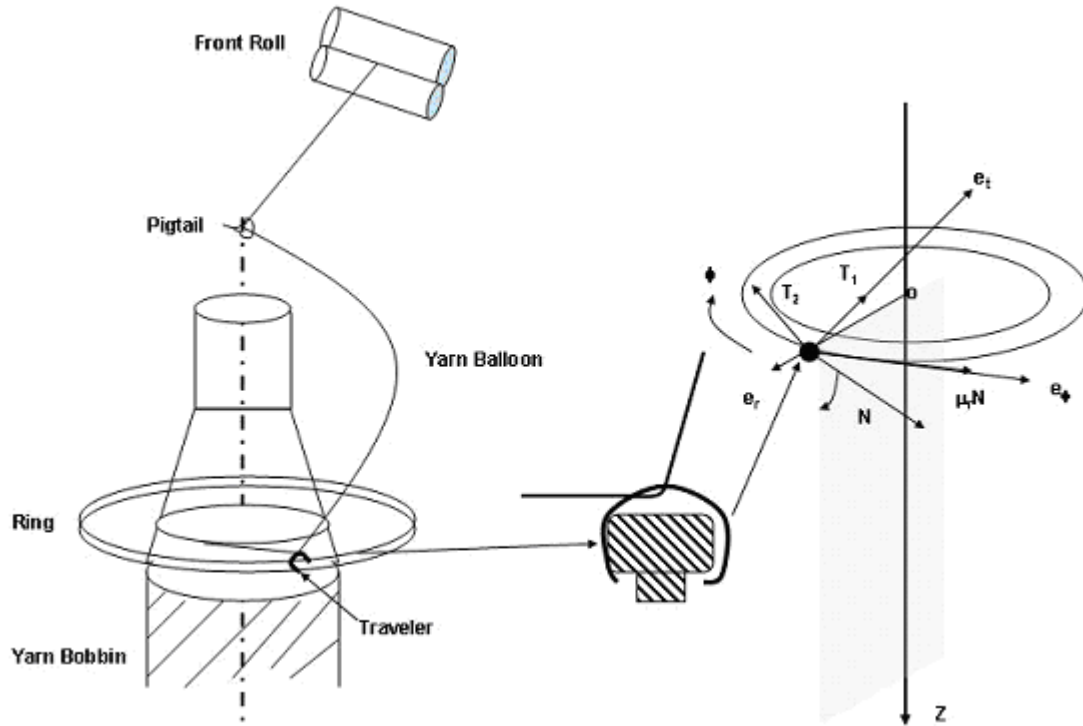


Figure 1. Different forces acting on the traveller [Betra et al, 4]

In this study, we developed a new spinning concept that takes advantage of all the quality features produced by ring-spinning, but with significant economical gains that are closely comparable with other high-production spinning systems. This concept is termed ‘magnetic spinning’, and it aims at completely eliminating the traveller concept and replacing it by magnetic rings. In this part of the study, we discuss the design of this system and the underlying concepts.

The concept of magnetic control

Magnetic spinning mainly consists of a lightweight rotor (Figure 2) suspended magnetically inside a fixed stator. The rotor can spin freely inside the stator. The stator is equipped with four magnetic actuators that always keep the rotor in its central position. The rotor in this configuration replaces the ring and traveller in the traditional spinning system.

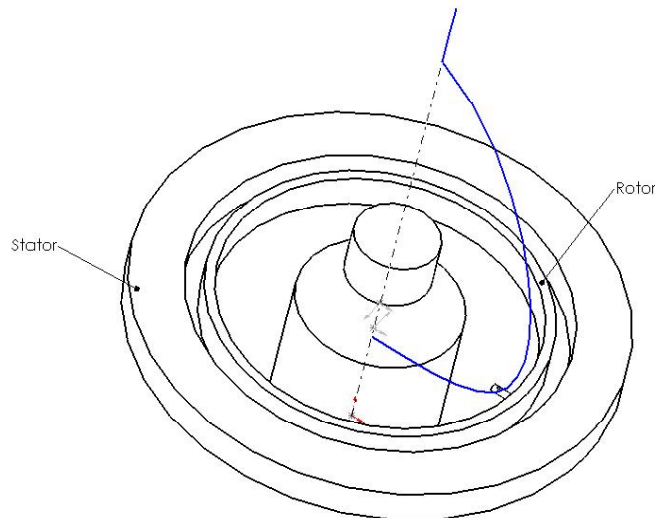


Figure 2. Magnetically suspended rotor in magnetic spinning

A completely passive and contact-free magnetic bearing that is stable in all 6 degrees of freedom (DOF) cannot be realistically constructed under normal conditions [9]. In practice, at least one axis has to be controlled actively by means of electromagnet actuators. Earlier publications on magnetic-bearing wheels aimed at controlling one, two or five DOF actively [2, 6, 11].

Magnetic levitation systems can be realised by using attractive or repulsive forces. A better mass/stiffness ratio can be achieved by using the attractive force mode [12]. Preference was given to the two DOF options where the wheel is actively controlled along two orthogonal radial directions, where axial movements and all other degrees of rotor freedom are passively controlled by means of permanent magnets, except for the rotor spin. The two radial axes are independently controlled by their control loops.

Both permanent magnets and electromagnetic coils are used in the system's design. Most of the DOFs are passively controlled. This has the advantages of high reliability and low power consumption because the amount of electronics is reduced. The permanent magnets produce the main part of the magnetic flux in the magnetic circuit, and the electromagnetic coils modulate this static bias flux, allowing the control of restoring forces on the rotor to keep it centred. This modulation is necessary to provide active control in the radial direction in the presence of imbalance or external forces. Another advantage is the linearised characteristic of force vs. current through the superposition of permanent magnetic and electromagnetic fluxes [14]. Rare-earth permanent magnets were chosen because they offer a high-energy density and have advantages in terms of mass and volume.

Principle of operation

Figure 3 shows a cross-section of the magnetic system. A bias flux is generated across the air gap (shown in blue paths from both permanent magnets), supporting the weight of the rotating disk in the axial direction. If the floating ring is displaced from its central position, the permanent magnets will create a destabilising force that attracts the ring even further away from the centre. The control system will read out this deviation from the centre position, using two displacement sensors mounted radially on the floating ring, and generate a current signal to the power amplifiers. The power amplifiers supply the electric coils with current to generate a corrective flux (shown in Figure 3 by the dotted path). This corrective flux subtracts and adds to the fluxes caused by the permanent magnets. By subtracting flux at the small gap side and adding flux at the large gap side, the total magnetic force will tend to bring the floating ring to its central position.

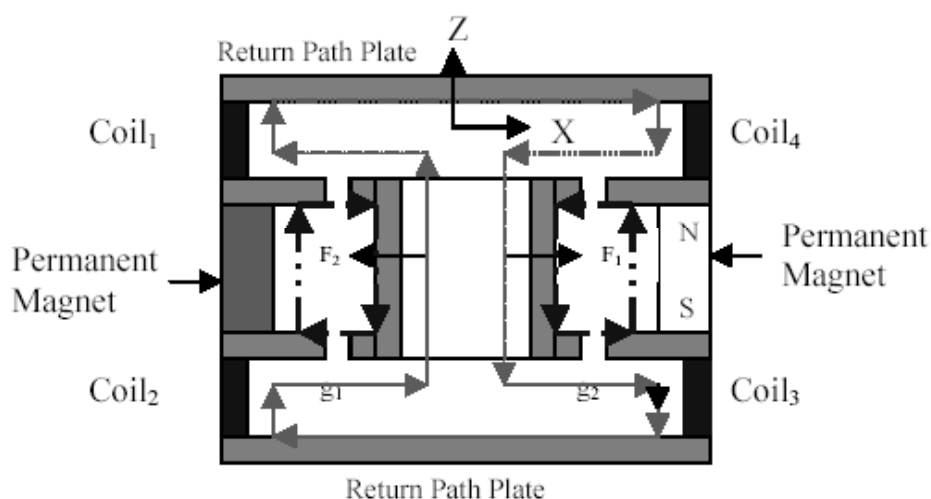


Figure 3. Cross-section of the magnetic system

Theoretical modelling of the system

The main aim of this study is to develop a theoretical model that helps in establishing a first trial control system, as well as how the system will respond to changing the control parameters. In this modelling, only one plane of movement is considered (X-Z plane Figure 3). The perpendicular plane

(Y-Z) is identical. Furthermore, it is assumed in this study that there is no flux leakage, and that the magnetic flux densities are below saturation, that is, that a linear B-H relation exists. We also assume that the field intensity in the cores is negligible due to the high permeability of the cores.

A. Field intensity

The field intensity of a permanent magnet H_p , in a gap g_i is equal to:

$$H_{g_i P} = -\frac{H_m l_m}{2g_i} \tag{1}$$

where g_i is the thickness of the gap i (where $i = 1, 2$), and (H_m, B_m) is the operating point of the permanent magnet, which can be found as explained in the next section.

B. Permanent magnet operating point

The load line (the equation that characterises the load behaviour of the permanent magnet load) is defined by the following equation:

$$B_m = -\mu_0 \frac{H_m l_m}{2g} \tag{2}$$

Solving this equation with the permanent magnet demagnetisation curve (the hysteresis loop) results in the operating point of the magnet. Since it is hard to solve it with the demagnetisation curve, we can solve it with a linearised equation of the demagnetisation curve at the suitable quarter of the (B-H) plane.

The approximate demagnetisation curve takes the following form:

$$B_m = B_r + \frac{B}{H_c} H_m \tag{3}$$

where B_r is the residual flux density and H_c is the coercive force of the permanent magnet. Figure 4 shows the solution of the two equations (2) and (3) (the intersections between the two lines).

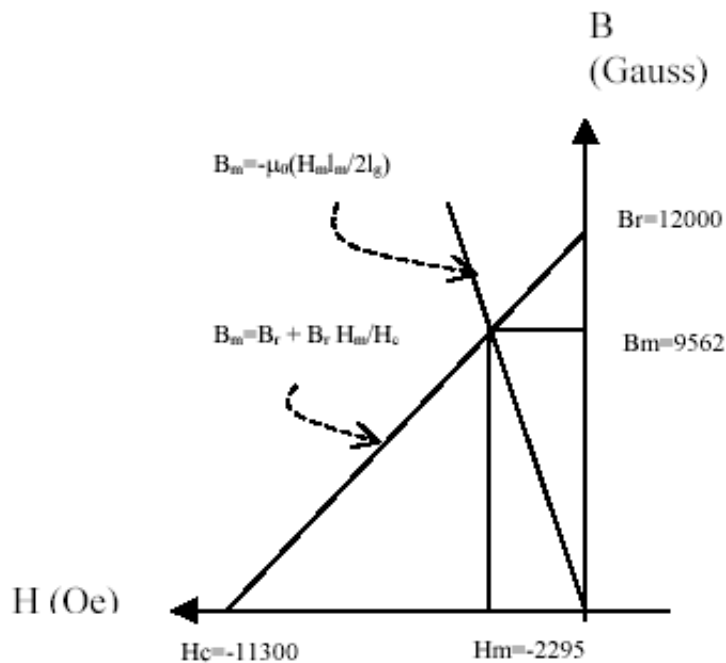


Figure 4. Finding the permanent magnet operating point

C. The field intensity in each gap due to the coils

The field in the gap due to coils 1 and 2 is calculated as follows:

$$2H_{gc} g_i = 2NI$$

$$H_{g_{ic}} = \frac{2NI}{g_i} \tag{4}$$

D. The total field intensity and force

The total field in each gap equals:

$$H_{g_i} = \frac{NI}{g_i} - \frac{H_m l_m}{2g_i} \tag{5}$$

The attracting force of each side equals:
From (4) in (5);

$$F_i = \frac{\mu_0 S}{g_i^2} \left(NI - \frac{H_m l_m}{2} \right)^2 \tag{6}$$

The total force acting on the rotor in x-direction:

$$F_{x-tot} = F_1 - F_2 = \mu_0 S \left[\left(\frac{NI - \frac{H_m l_m}{2}}{g_1} \right)^2 - \left(\frac{NI + \frac{H_m l_m}{2}}{g_2} \right)^2 \right] \tag{7}$$

Let $g_1 = \Delta - x$, hence, $g_2 = \Delta + x$, see Figure 4.

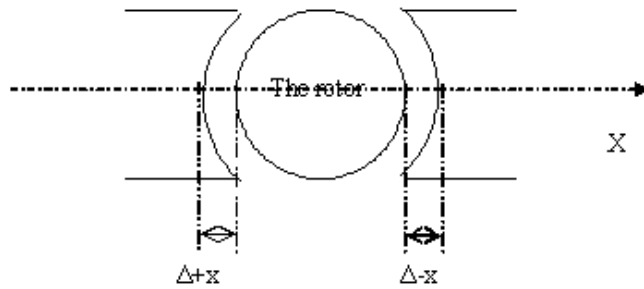


Figure 5. Schematic top view of the rotating ring and two flux segments

Also, let $H_m l_m = 2NI_m$, (as if the permanent magnet has been replaced with a coil with N_m turns and I_m DC current.

Using these two quantities, Equation 7 can be rewritten as:

$$F_{x-tot} = \mu_0 S N \left(\frac{I_m}{\Delta} \right)^2 \left[\left(\frac{1 - \frac{I}{I_m}}{1 - \frac{x}{\Delta}} \right)^2 - \left(\frac{1 + \frac{I}{I_m}}{1 + \frac{x}{\Delta}} \right)^2 \right] \tag{8}$$

Equation 8 can be approximated as:

$$F_{x-tot} = K \left(\frac{I}{I_m} + \frac{x}{\Delta} \right) \tag{9}$$

Control engineering aspects

This newly developed system requires active control in two radial axes because of the inherent instability in these directions. Four sensors are inserted into the stator body to measure the distance of the rotating ring in differential mode. These sensors are inductance sensors that change their inductance, using a 30 kHz carrier signal, with the change in the distance of the target surface (floating ring) from the sensor. In order to realise a control system capable of stabilising the rotating ring during spinning, a complete block diagram of the system has to be constructed first. The main element of the system is the dynamic of the rotating ring.

The transfer function of the rotating ring

The differential equation that describes the rotating ring is:

$$\begin{aligned}
 mx'' &= F_{x-tot} + f(t) \\
 mx'' &= K\left(\frac{I}{I_m} + \frac{x}{\Delta}\right) + f(t)
 \end{aligned}
 \tag{10}$$

where $f(t)$ describes any disturbance force acting on the floating ring (in our case, the yarn tension is considered as a disturbing force), and K is a constant depending on the system parameters.

Taking the Laplace transform for both sides of the equation (10), and neglecting the disturbance term $f(t)$:

$$\begin{aligned}
 mXs^2 &= 4K\left(\frac{I}{I_m} + \frac{X}{\Delta}\right) \\
 X\left(\frac{ms^2}{4K} - \frac{1}{\Delta}\right) &= \frac{I}{I_m} \\
 \frac{X}{I} &= \frac{1}{\frac{mI_m}{4K}s^2 - \frac{I_m}{\Delta}}
 \end{aligned}
 \tag{11}$$

The transfer function 11 has two poles on the right-hand side of the S plane which indicates instability. To overcome this situation, some other blocks have to be inserted in the feedback path. These blocks represent the following elements:

The displacement sensor

The first block in the feedback circuit is the displacement sensor conversion factor. For linear displacement sensor it is the constant K_s and equals the ratio between the displacement sensed and the output voltage of the sensor. A low pass filter is put with the sensor, and the resulting transfer function is:

$$\frac{K_s}{\tau_1s + 1}$$

The compensation circuit

A PID (Proportional-Integral-Derivative) controller is used, which has a transfer function of the form: $K_p + K_Ds + \frac{K_I}{s}$, where K_p , K_D , and K_I are the proportional, the derivative, and the integral gains respectively. The function of the controller is to achieve the stability of the system, that is, it maintains the ring's central position.

Gain

The current stiffness gain K_i is added in the feedback loop as another control factor to increase the response speed.

Figure 6 shows the overall proposed control loop to maintain the stability of the rotor during spinning.

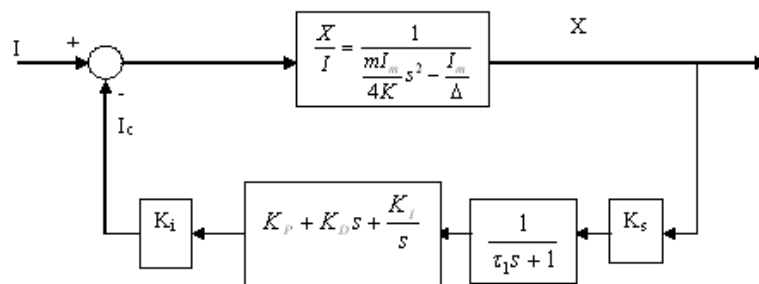


Figure 6. Diagram of the control system

Simulation

A model of the system has been build using Simulink® software, as shown in Figure 7; in this model the main components are the ring, which is simulated as a body with two degrees of freedom, and the yarn, which is simulated using a finite number of small cylindrical objects connected together with spherical joints to ensure their freedom of movement; both the radius and density rods are of values similar to a normal yarn. The ring is kept rotating in the simulation using two quadratic signals (sine and cosine waves). Air drag is also taken into account, and is simulated as an opposing force to both the ring and the yarn (the force depends on the speed and the characteristics of the ring and the yarn). A full description of the model, the simulation and its outputs is introduced in a separate paper [1].

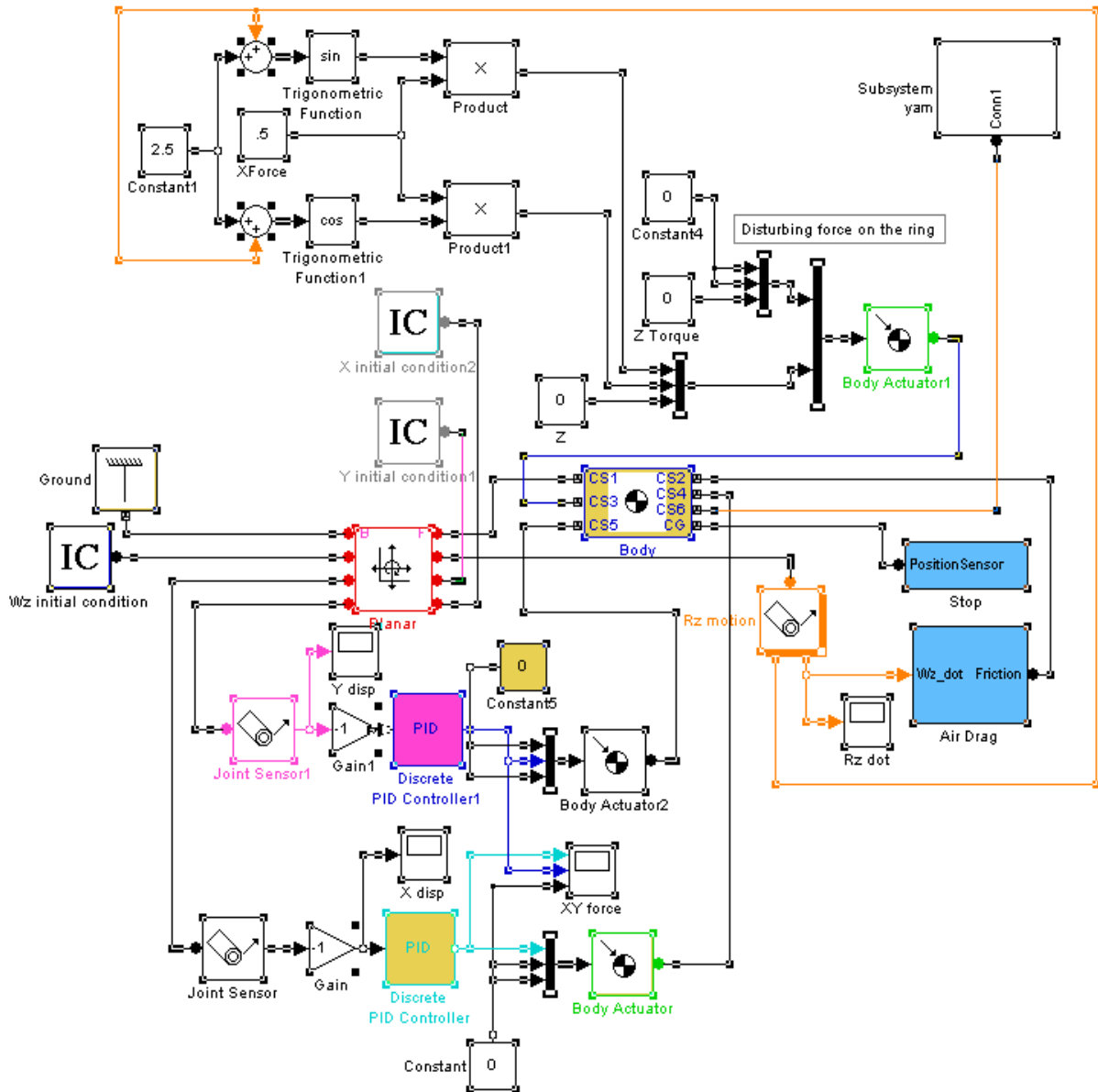


Figure 7. Simulink model

The system was simulated with different PID parameters, and the simulation showed that the system model is valid and the system can reach stability within 700 ms. Figure 8a shows a top view and a 3D view of the yarn balloon while in a transitional state (at the beginning of the motion), while Figure 8b shows a top view and a 3D view of the yarn balloon after reaching stability. In these figures, the red triangle represents a section in the ring plane.

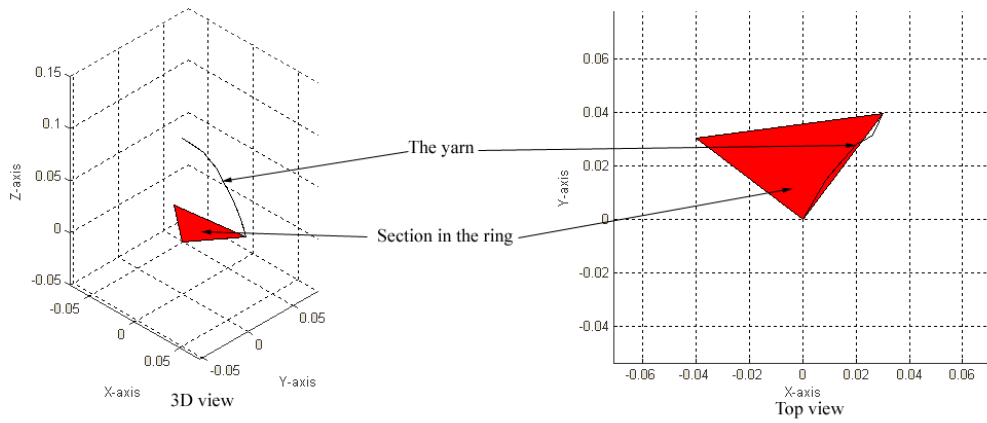


Figure 8a. Yarn balloon in a transitional state – 3D and top view (at 1.5 ms after starting simulation)

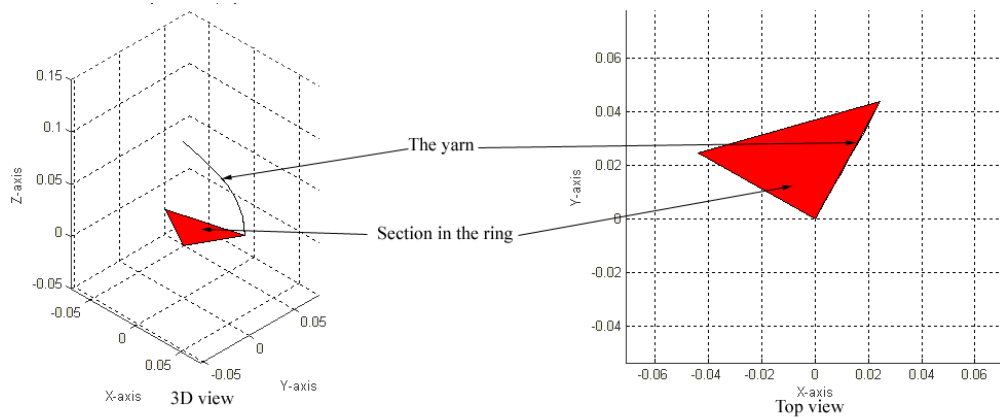


Figure 8b. Yarn balloon at steady state – 3D and top view (700 ms after starting simulation)

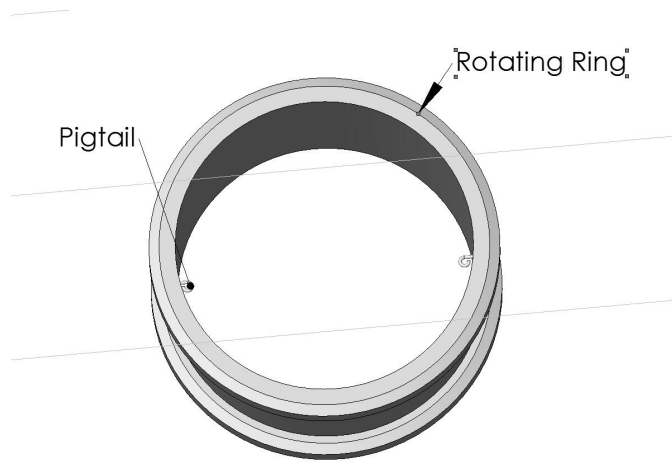


Figure 9. Detail of rotating ring, showing the pigtail for yarn path

Conclusions

A new ring-spinning concept named ‘magnetic spinning’ is introduced; the system is based on magnetic suspension, where a lightweight rotor is designed to be magnetically suspended inside a fixed stator, using electromagnets that modulate the field of radially-mounted permanent magnets to keep the rotor suspended, displacement sensors to sense the position of the rotor, and a control circuit to adjust the electromagnets’ input current based on the position. The system has been modelled and simulated using Simulink® software, and the simulation demonstrated the validity of the concept. Figure 9 shows the detailed configuration of the rotating ring. A prototype of the system has been built and is being tested, and is shown in Figure 10.

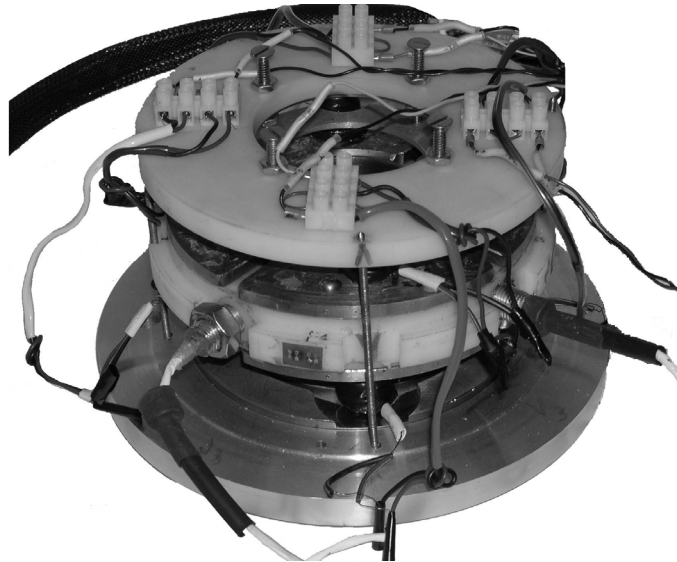


Figure 10. A picture of the prototype

References:

1. Abdel-Hady, F., and Abuelenin, S. M.: "Numerical simulation of magnetic ring spinning process", AUTEX world textiles conference, Slovenia, 2005
2. Anstett, P., Souliac, M., Rouyer, C., Gauthier, M.: "SPOT - The Very First Satellite to Use Magnetic Bearing Wheels", 33rd IAF Congress, Paris, France 1982.
3. Artzt, P.: "Compact Spinning – A True Innovation in Staple Fibre Spinning", ITB, No. 5, PP 26-32, 1998.
4. Batra, S. K., Ghosh, T. K., and Zeidman, M. I.: "An Integrated Approach to Dynamic Analysis of the Ring Spinning Process Part I: Without air Drag and Coriolis Acceleration", Textile Res. J. 59(6), 309-317 (1989)
5. Batra, S. K., Ghosh, T. K., and Zeidman, M. I.: "An Integrated Approach to Dynamic Analysis of the Ring Spinning Process Part II: With air Drag", Textile Res. J. 59(7), 416-424 (1989)
6. Bichler, U., Eckart, T.: "A Gimbaled Low Noise Momentum Wheel", 27th Aerospace Mechanisms Symposium, NASA Ames Research Centre, May 1993.
7. De Barr, A. E., A Descriptive Account of yarn Tensions and Balloon Shapes in Ring Spinning, J. Textile Inst. 49, T58, 1958.
8. Deussen H.: "Rotor Spinning Technology", Book Published by Schlafhorst Inc., Charlotte, NC, U.S.A. 1993.
9. Earnshaw, S.: "On the nature of molecular forces which regulate the constitution of the limiferous ether", Trans. of the Cambridge Philosophical Society Vol. 7, 1842.
10. El Mogahzy, Y. E., and Chewning, C. H., "Cotton Fibre To Yarn Manufacturing Technology: Optimizing Cotton Production By Utilizing The Engineered Fibre Selection® System", Book Published by Cotton Incorporated (Cottoninc.com), 2001.
11. Robinson, A.A.: "A Light-Weight, Low-Cost, Magnetic-Bearing Reaction Wheel for Satellite Attitude Control Applications", ESA Journal, Vol. 6, 1982.
12. Roland, J.P.: "Magnetic Bearing Wheels for Very High Pointing Accuracy Satellite Missions", International Symposium on Magnetic Suspension Technology, Hampton, Virginia, 1991. NASA Conference Publication 3152.
13. Skenderi, Z., Oreskovic, V., Peric, P., and Kalinovic, H.: "Determining Yarn Tension in Ring Spinning", Textile Res. J. 71 (4), 343-350, 2001
14. Studer, P.A., Allaire, E.H., Sortore, C.K.: "Low Power Magnetic Bearing Design for High Speed Rotating Machinery", International Symposium on Magnetic Suspension Technology, Hampton, Virginia, 1991. NASA Conference Publication 3152.

▽△